A compact, exchangeable and fast-cooling cryogenic system for HTS antennas

HW. Zhang[1,2], HM. Liu[1*], ZR. Zhou[1,3], YQ. Zhao[1], YM. Han[1], FY. Chen[1], Z. Geng[1,2], D. Jiang[1,2], RJ. Huang[1,2] and Y. Zhou[1,2]

[1] State Key Laboratory of Cryogenic Science and Technology, Technical Institute of Physics and Chemistry, Chinese Academy of Sciences, Beijing 100190, P. R. China
[2] University of Chinese Academy of Sciences, Beijing 100049, P. R. China
[3] Hunan Key Laboratory of High-Performance Intelligent Sensor and Detection System, The 48th Research Institute of CETC, Changsha 410111, P. R. China

[*]E-mail: huimingliu@mail.ipc.ac.cn

Abstract: This paper explores the cooling demands of high-temperature superconducting microwave receiver front-ends, specifically aiming at microstrip antennas within a cryogenic subsystem. Firstly, a transient heat transfer model was developed based on experiments with a 3 W @ 77 K pulse tube cryocooler. Then, a cryogenic system with a 15 W @ 77 K cryocooler was designed from this model, achieving a cooling time to 75 K of 17 minutes and a minimum temperature below 50 K, after optimization of heat transfer paths and interface thermal resistance. Furthermore, a thermo-mechanical coupling structure was designed to facilitate rapid cryocooler replacement without compromising the devices' vacuum environment. This configuration allows the antenna to reach 75 K in 22 minutes, with a minimum temperature below 55 K. The research contributes valuable insights for the design and optimization of cryogenic subsystems in high-temperature superconducting microwave receiver front-ends.

1. Introduction

High-temperature superconducting (HTS) materials exhibit microwave surface resistance 2–3 orders of magnitude lower than conventional metals. Devices fabricated from these materials demonstrate high Q-factors and low microwave losses, making them highly promising for applications in radar systems, telecommunications, and satellite technologies. However, as microwave receiver front-ends advance toward higher power handling, multi-channel operation, and all-HTS configurations, there is an urgent need for compact, fast-cooling and reliable cryogenic subsystems [1,2].

Previous research mainly focused on the circuit design of HTS microwave devices and their communication performance testing under steady-state temperatures (usually at LN_2 temperatures, which are below the superconducting transition temperature of YBCO thin films), while neglecting the transient cooldown time [3,4]. Some studies have explored strategies such as adjusting voltage or frequency to reduce the cooldown duration of pulse tube cryocoolers (PTCs) . However, these investigations are limited to the cryocooler itself as a standalone cold source, without accounting for the integrated system's transient thermal behavior—for instance, computational models often overlook material property variations and radiative heat leakage in coupled device-cryocooler systems [5,6].

Content from this work may be used under the terms of the Creative Commons Attribution 4.0 licence. Any further distribution of this work must maintain attribution to the author(s) and the title of the work, journal citation and DOI.
Published under licence by IOP Publishing Ltd

Regarding cold source reliability, Duan et al. [7] proposed a dual-cryocooler backup system, consisting of two independent vacuum chambers and cryocooler units. If one unit fails, the other can be rapidly activated—significantly improving system reliability but at the cost of doubled expense, volume, and weight. Alternatively, some researchers have introduced plug-and-play cryocooler-dewar structures, allowing for cryocooler replacement upon failure. However, this design struggles to simultaneously optimize thermal contact and mechanical fit, necessitating further improvements to achieve low heat leakage, flexible connections and adjustable vacuum level.

In this paper, a transient heat transfer simulation model was first proposed and validated with experimental data from the cryogenic antenna system based on a 3 W @ 77 K PTC. Then, the cooling performance of the cryogenic subsystem with a 15 W @ 77 K PTC was predicted using this model, and its optimized cooldown time and steady-state temperature were verified through experimental testing. Finally, a quick-exchange cryocooler mounting structure (QECMS) was designed to ensure both thermal conduction and mechanical coupling, and the impact of its vacuum level on system performance was examined.

2. Numerical simulation

2.1 Basic model and governing equations

A typical HTS antenna cryogenic system is shown in Figure 1. The cooling power is provided by a low-vibration pulse tube cryocooler cold head, which extracts heat from the target components (HTS microstrip antenna and cryogenic low-noise amplifier (LNA)) through a cold finger and cold plate, thereby maintaining them at cryogenic temperatures. Coaxial lines connect the microwave components (cryogenic temperature) to the vacuum chamber wall (room temperature) for signal transmission, and the radome achieves electromagnetic wave transmission while simultaneously maintaining vacuum insulation.

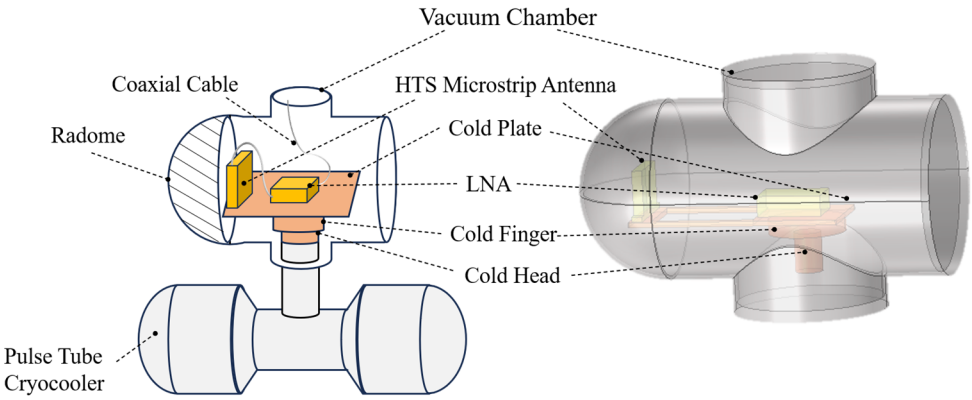

Figure 1. A typical cryogenic system for HTS antennas (*L:* Schematic; *R:* Simulation geometry).

In the simulation software COMSOL Multiphysics, the model was appropriately simplified to reduce computational complexity: (1) The antenna and LNA were modeled as solid brass blocks. (2) Only the cold head section of the cryocooler was included. (3) The conductive heat leakage of the coaxial cable was added as a boundary heat source on the device walls. (4) The inner wall coating of the radome was assumed to have identical material properties to the vacuum chamber

wall. (5) All external surfaces were set to a constant room temperature of 300 K. (6) The effect of heat convection was neglected.

The governing equations for the transient heat transfer simulation model are as follows:

$$\rho c_p \frac{\partial T}{\partial t} + \nabla \cdot (-k\nabla T) = -Q_c + Q_b + Q_r \tag{1}$$

$$Q_c = aT + b \tag{2}$$

$$Q_b = \frac{A}{L}\int_{T_c}^{T_h} k(T)\, dT \tag{3}$$

$$Q_r = \frac{A_c\sigma\left(T_h^4 - T_c^4\right)}{\left(\frac{1}{\varepsilon_c} - 1\right) + \frac{1}{F_{c-h}} + \frac{A_c}{A_h}\left(\frac{1}{\varepsilon_h} - 1\right)} \tag{4}$$

where ρ, c_p, T, t, k denote material density (kg/m^3), specific heat capacity (J/kg·K), temperature (K), time (s) and thermal conductivity (W/m·K), respectively. The right-hand side of Equation (1) sequentially includes cooling capacity of the cryocooler Q_c (W), conductive heat leakage of the coaxial cable Q_b (W) and radiative heat leakage Q_r (W). In Equation (2)-(4): a, b denote numerical constants in the fitting function (dimensionless); A, L represent cross-sectional area (m^2) and characteristic length (m), respectively; σ is the Stefan-Boltzmann constant (5.67×10^{-8} W·m^{-2}·K^{-4}); ε indicates surface emissivity; F stands for the view factor between surfaces (dimensionless). Subscripts c and h represent the cold side and hot side, respectively.

2.2 Model validation

To validate the simulation model, experimental cooling data from a previously constructed cryogenic system were used for comparison. The cold source was LIHAN TC3380 PTC (3 W @ 77 K nominal cooling capacity with a fitted curve Q_c = 0.1023*T – 5.11162 (W)). The curve was derived from a linear regression analysis based on the technical datasheet. The cold finger (φ 45×8 mm) and cold plate (123×50×3 mm, with a 60×40 mm cutout near the antenna section) were made from oxygen-free copper (OFC). The HTS antenna (35×29×6 mm) and LNA (38×25×12 mm) were cooled from room temperature (300 K), with Cu-PTFE-Cu coaxial cables (φ 1.2×200 mm) on their walls. Temperature-dependent material properties from the NIST database were taken into account, and all surfaces inside the vacuum chamber were assumed to have an emissivity of 0.1.

As shown in Figure 2, the simulation results are in good agreement with experimental data, with a maximum deviation of less than 6%, validating the model's accuracy. However, the cooldown time to 75 K exceeds one hour (greater than the 30-minute demand for practical use), and the steady-state temperature stabilizes around 65 K, indicating the need for further optimization.

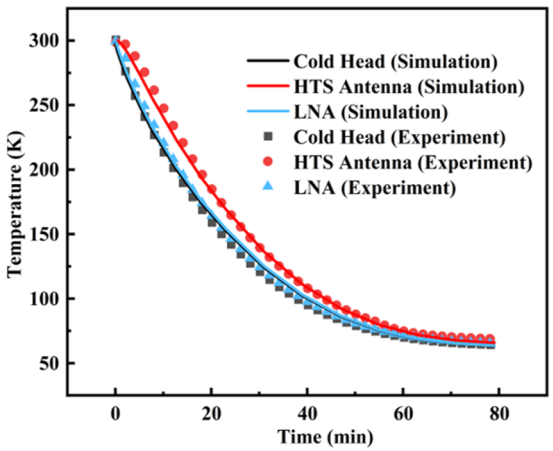

Figure 2. Comparison between simulation and experiment results (3 W PTC).

2.3 Optimization of cooling performance

Equation (1) reveals that the cooling performance of the cryogenic system can be enhanced through three aspects: optimizing heat transfer paths, increasing the cooling capacity of the cryocooler, and minimizing heat leakage. However, given the electromagnetic shielding effects of radiation barriers and spatial/transmission constraints on coaxial cables, our optimization primarily focused on the first two approaches.

The optimized system utilized the LIHAN TC4188 PTC (15 W @ 77 K) as the new cold source, with $Q_c = 0.334*T - 9.55131$(W). The heat transfer paths' optimization was conducted on the cold finger and cold plate. For the cold finger design, four sector-shaped sections with radius r (r = 0.1 ~ 14 mm) and depth h (h = 0.1 ~ 7 mm) were removed from the perimeter. The cold plate modification involved adjusting the length m (m = 50 ~ 60 mm) and width n (n = 25 ~ 47.5 mm) of the cutout portion, as illustrated in Figure 3(a). Although removing these non-essential sections reduced thermal mass, it simultaneously decreased the available heat transfer area. To balance these competing factors, the Nelder-Mead algorithm was employed to optimize these four parameters (r, h, m, n). The optimization objective was set to minimize the antenna temperature within 15 minutes, achieving optimal cooling performance while maintaining structural integrity.

Figure 3(b) compares the cooldown time to 75 K between the original and optimized designs for the cold head, antenna, and LNA, with the optimized parameters r, h, m, n set at 13, 7, 50, 30 (mm), respectively. Taking the antenna as an example, the optimized design achieves a projected cooldown time of 16 minutes to reach 75 K, representing a 73.33% reduction compared to the baseline configuration. The final steady-state temperatures for all components are maintained below 50 K, demonstrating significant optimization effectiveness. These promising simulation results represent an optimal balance between thermal mass and heat transfer efficiency, which will guide the construction of an experimental platform to validate the optimized design.

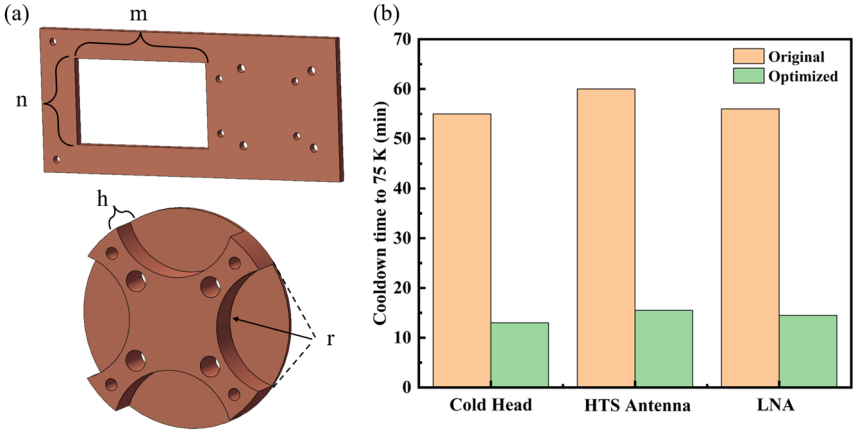

Figure 3. (a) Optimized parameters; (b) Cooldown time to 75 K: original vs. optimized design.

3. Experimental investigation

3.1 Apparatus and procedures of the experiment

Based on the simulation optimization results, a new cryogenic antenna system was designed and an experimental setup was constructed to test its cooling performance. Figure 4 shows the schematic view.

The cryogenic system (outlined in yellow) has compact dimensions of 300 × 220 × 360 mm and a total weight of <12 kg. The stainless steel vacuum chamber features a KF flange on the upper port for vacuum pump connection to achieve high vacuum (<10^{-5} Pa). SMA connectors are also installed for 1.2mm coaxial cable routing, simulating realistic thermal leakage conditions. Inside the chamber, an HTS antenna and LNA module (both fabricated from brass blocks) are mechanically bolted to the heat transfer structure, which consists of the simulation-optimized OFC components mounted on the LIHAN TC4188 PTC (15 W @ 77 K) cold head. The cryocooler and control electronics are powered by a switching power supply, housed in a rack-mount enclosure with forced-air cooling. PT100 temperature sensors (calibrated range: 30 ~ 320 K, accuracy: ±0.1 K) are attached with GE varnish to the antenna, LNA, and cold head, with data acquisition managed by a temperature controller. Signal transmission is routed through a side-mounted KF flange. System-wide control and data processing are handled by a host computer.

During the experiment, the vacuum chamber was first evacuated to a pressure below 10^{-3} Pa at room temperature using the vacuum pump. Once the target vacuum level was achieved, the cryocooler and temperature controller were activated to initiate the cooling process while continuously monitoring system parameters. After reaching thermal equilibrium, the cryocooler was powered off to allow the system to warm back to room temperature. Throughout this process, key parameters including temperature distribution, vacuum level, and input power were recorded in real-time to characterize the system's thermal performance. It is also worth noting that indium foil and Apiezon N grease were applied as thermal interface materials (TIMs) at all contact surfaces to minimize heat transfer loss. Additionally, the cold plate and cold finger were integrated into a monolithic component to significantly reduce interface thermal resistance. These improvements are illustrated in Figure 5.

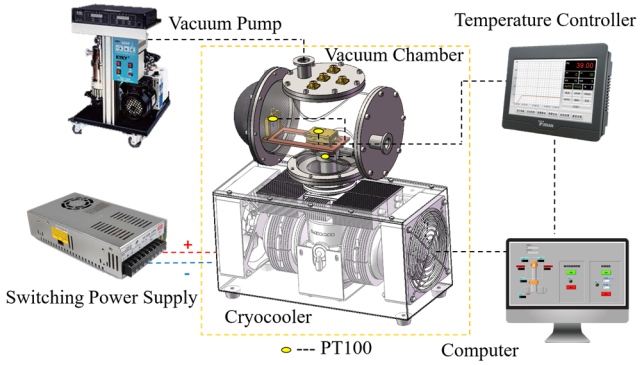

Figure 4. Schematic view of the experimental setup.

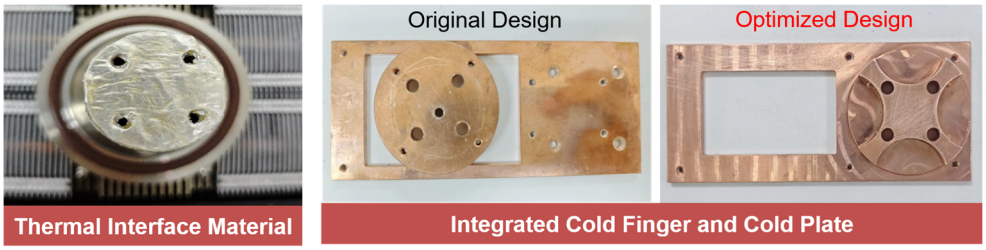

Figure 5. Detailed improvements to reduce cold loss.

3.2 Cooling performance of the optimized design

Figure 6(a) shows the cooldown curve of the optimized cryogenic antenna system, with the cold head, HTS antenna, and LNA reaching 75 K in 14.85 min, 16.65 min, and 16.15 min, respectively. The system achieved thermal equilibrium below 50 K, with the antenna and LNA maintaining approximately 45 K at steady-state. The experimental results match simulations well, with minor deviations likely caused by heat source modeling errors and interface thermal resistance. This demonstrates the system's fast-cooling capability, meeting demands for HTS microwave receiver front-ends (<30 min).

A comparative analysis of three optimization stages for the HTS antenna cooling results is presented in Figure 6(b). The implementation of a higher-capacity PTC cryocooler reduced the 75 K cooldown time from 60 min to 23 min (61.67% improvement). Subsequent thermal paths' optimization further decreased this duration to 18 minutes (an additional 21.74% enhancement, based on the same 15 W PTC), while interface improvements achieved a final reduction to under 17 minutes (7.22% gain). Corresponding steady-state temperatures demonstrated progressive improvement from 69 K to 45 K (34.78% total reduction). These results indicate significant enhancements in both transient and steady-state performance, with the cryocooler's cooling capacity exhibiting the most substantial impact. However, practical implementation requires comprehensive consideration of the increased cost, weight, and volume associated with higher-capacity cooling systems.

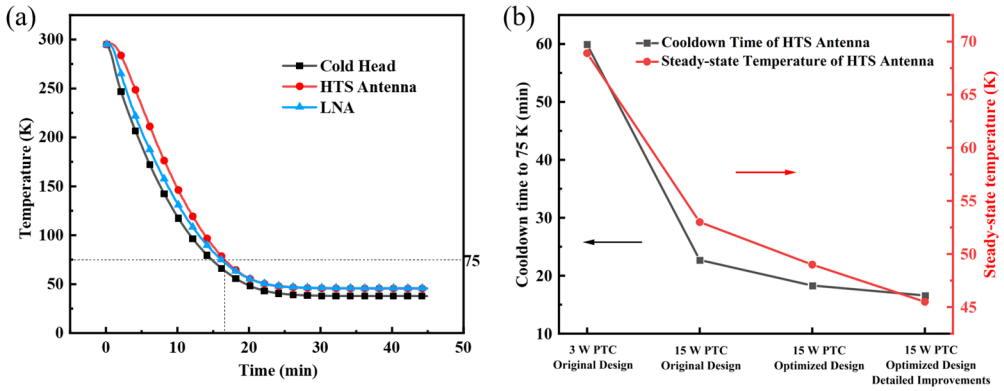

Figure 6. (a) Cooldown curve of the optimized design after detailed improvements (15 W PTC); (b) Cooldown time and steady-state temperature of HTS antenna under different working conditions.

3.3 Quick-exchange cryocooler mounting structure (QECMS)

To ensure cooling source reliability, we designed a rapid cryocooler replacement structure that integrates both thermal contact and mechanical compatibility, as illustrated in Figure 7. The male OFC transition piece is mounted on the cryocooler cold head and achieves efficient heat transfer through threaded coupling with its female counterpart, which connects to the device chamber's cold plate. The stainless steel inner and outer cylinders isolate the device chamber from the QECMS chamber while extending the thermal path to minimize conductive heat leakage. A flexible bellows, welded to both upper and lower stainless steel transition pieces, provides hermetic sealing and axial compliance, further reducing heat transfer. The system employs a KF flange connection with the cryocooler and incorporates a stainless steel evacuation tube for vacuum regulation. Adjustable nuts on threaded rods precisely control bellows compression for optimal

thermal-structural coupling, while fixed nuts prevent deformation during maintenance due to pressure differentials.

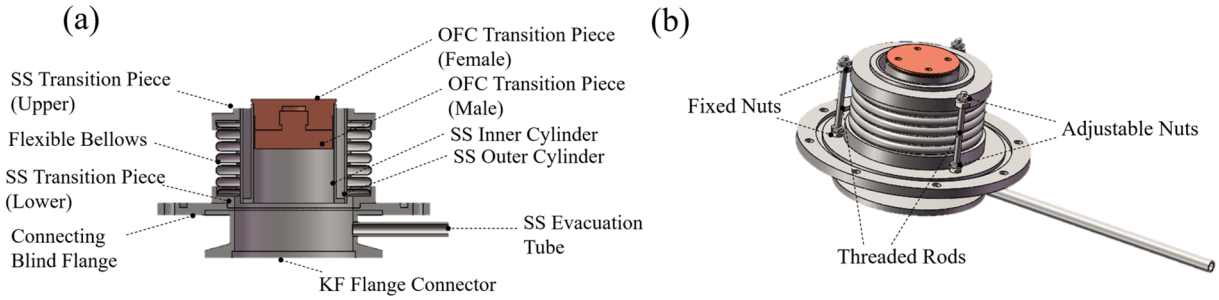

Figure 7. Quick-exchange cryocooler mounting structure (SS: stainless steel; OFC: oxygen-free copper). (a)Cross-sectional view; (b) Schematic of external appearance.

Figure 8 presents the cooling-replacement-recooling curve of the cryogenic antenna system with QECMS. Though the parasitic heat loads of the replacement structure increased the cooldown time to approximately 22 minutes and elevated the steady-state temperature to around 50 K, the system still achieved the target operating temperature within 30 minutes. The replacement procedure with a new cryocooler was completed within several minutes, during which the device temperature rose to 161 K. Then, the system re-cooled to the 75 K operating temperature. The whole replacement and recooling process took 18.92 minutes. These experimental results confirm the operational effectiveness of the rapid cryocooler replacement structure, demonstrating its capability to maintain system functionality.

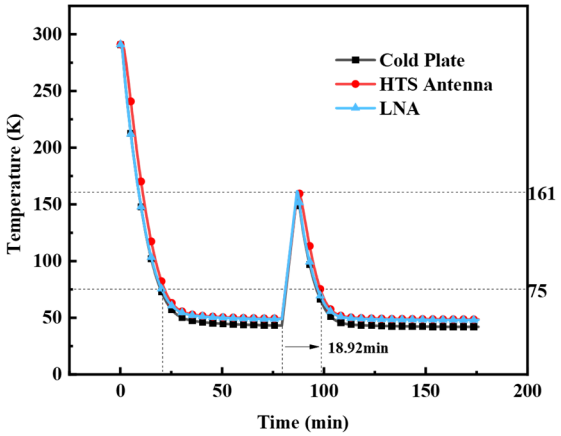

Figure 8. Cooling-replacement-recooling curve of the cryogenic antenna system with QECMS.

Considering that each replacement would disrupt the vacuum in the QECMS, we investigated the impact of vacuum levels on overall cooling performance, summarized in Table 1. Experimental results indicate that vacuum pressures between $10^3 \sim 10^5$ Pa significantly affect cooldown time, while pressures between $10^{-1} \sim 10^1$ Pa notably influence steady-state temperature. The heat transfer mechanism of residual gas within the QECMS structure warrants further study [8]. Nonetheless, maintaining vacuum pressure below 10^3 Pa allows cooling to 75 K within 22

minutes, with a steady-state temperature below 55 K, which is acceptable for practical applications and can be achieved using portable micro-pumps.

Table 1. Cooling results of HTS antenna under different vacuum levels in the QECMS.

Results of HTS antenna	$< 10^{-1}$ Pa	10^{1} Pa	10^{3} Pa	10^{5} Pa
Cooldown time to 75 K	21.34 min	21.99 min	22.17 min	23.49 min
Steady-state temperature	48.71 K	52.82 K	53.42 K	53.90 K

4. Conclusion

This study developed a transient heat transfer model based on experimental data from a 3 W @ 77 K PTC. Using this model, the cooling performance of a cryogenic antenna system was optimized and validated through experiments. The results demonstrate that after adopting a 15 W @ 77 K PTC and optimized heat transfer paths, the HTS antenna could achieve a cooldown time to 75 K in 17 minutes with steady-state temperatures below 50 K. Furthermore, a rapid cryocooler replacement structure was designed, which maintains efficient thermal and mechanical coupling while enabling cryocooler replacement within minutes. This modified system retains satisfactory performance (22-minute cooldown time to 75 K and steady-state temperature <55 K), though the heat transfer mechanism of residual gas within the structure requires further investigation. The work provides practical solutions for implementing HTS microwave front-ends in applications demanding both thermal performance and operational flexibility.

Acknowledgements

This work was supported by the National Key Research and Development Program of China (No. 2023YFF0721302) and the China Postdoctoral Science Foundation (No. 2024M753314).

References

[1] Li C-G et al. 2021 *Acta Phys. Sin.* **70** 018501
[2] Du J, Wang J, Zhang T, Bai D, Guo Y J and He Y 2015 *IEEE Trans. Appl. Supercond.* **25** 1–4
[3] Wang L T, Xiong Y, Xiao Y H, Liu J Y, He M, Chen H H, Ji L, Zhao X J and Song F B 2019 *J. Supercond. Nov. Magn* **32** 2849–56
[4] Zeng X, Huang K, Hu Z, Chen Q and Xiao W 2017 *Int. J. Antennas Propag.* **2017** e6035202
[5] Yan C, Dai W, Wang Y, Wang X, Pfotenhauer J M, Zhang Y, Li H and Luo E 2021 *Int. J. Refrig.* **130** 99–103
[6] Wang B, Li R, Chao Y, Zhuang C, Zhao Q, Sun S, Yan C and Gan Z 2023 *Int. J. Refrig.* **150** 304–12
[7] Duan Y, Wang J, Wang W, Wu S, Qi H, Wang Z, Fang C, Huang R, Li L and Zhou Y 2022 *Sci. China Technol. Sci.* **65** 735–9
[8] Volschenk G, O'Shea M and Shaughnessy B 2024 *Cryogenics* **144** 103946